Am J Transl Res 2021;13(6):7193-7199
www.ajtr.org /ISSN:1943-8141/AJTR0128442

Original Article

Correlation analysis between rim enhancement features of contrast-enhanced ultrasound and lymph node metastasis in breast cancer

Yanling Guo, Qingfei Song, Qiaohong Pan

Department of Ultrasound Medicine, Heping Hospital Affiliated to Changzhi Medical College, Changzhi, Shanxi, China

Received December 17, 2020; Accepted February 9, 2021; Epub June 15, 2021; Published June 30, 2021

Abstract: Objective: To explore the correlation between rim enhancement features of contrast-enhanced ultrasound and lymphatic metastasis, and to provide theoretical support for clinical treatment of breast cancer. Methods: 387 breast cancer patients (748 axillary lymph nodes in total) treated in our hospital from January 2017 to January 2020 were selected and analyzed by contrast-enhanced ultrasound. Pathological examination showed that 540 axillary lymph nodes showed metastasis whereas 208 axillary lymph nodes did not show metastasis. Univariate analysis and Logistic stepwise regression were used to analyze the correlation between rim enhancement features of contrast-enhanced ultrasound and axillary lymph node metastasis of breast cancer. Results: Peripheral halo, peripheral convergence, rim enhancement, enhancement mode, enhancement amplitude, enhancement sequence, expansion after enhancement, peak intensity, time to peak, area under curve, thrombolysis in myocardial infarction, perfusion sequence, aspect ratio, and maximum cortical thickness were all related to lymph node metastasis of breast cancer by univariate analysis, and the difference was statistically significant ($P < 0.05$). Multivariate analysis showed that enhancement mode, enhancement amplitude, extension after enhancement, maximum cortical thickness, peak intensity and time to peak were all related to lymph node metastasis of breast cancer. Conclusion: Rim enhancement features of contrast-enhanced ultrasound of breast cancer are related to lymph node metastasis, which will provide a guidance for clinical treatment of breast cancer.

Keywords: Breast cancer, contrast enhanced ultrasound, lymph node metastasis, relevance

Introduction

Breast cancer (BC) is a malignant tumor with the highest incidence among common female diseases, which seriously affects the physical and mental health and even endangers the lives of the patients [1-4]. According to relevant reports, the incidence of BC accounts for 7%-10% of malignant tumors, and it mostly occurs in middle-aged and elderly women [4, 5]. However, in recent years, the incidence has increased year by year, and it gradually begins to affect the younger generation. Axillary lymph node is an important path of BC lymph node metastasis, which serves as a crucial basis in selecting treatments and evaluating prognosis in clinic [5-8]. Ultrasonic contrast is a highly accurate and non-invasive examination method, which can predict whether BC lymph node metastasis occurs according to imaging analysis. Based on this, in this study, the correlation between rim enhancement features of contrast-enhanced ultrasound (CEUS) and lymph node metastasis of BC was explored by analyzing the rim enhancement features of axillary lymph nodes of BC, so as to provide a reference for clinical treatment of BC.

Materials and methods

General data

387 patients with BC admitted to our hospital for treatment from January 2017 to January 2020 were selected. All the objects enrolled were female, aged from 31 to 76 years old, with an average age of (50.4 ± 3.5) years old, including 341 cases of invasive ductal carcinoma (IDC) and 46 cases of ductal carcinoma in situ (DCIS). All patients received the CEUS for

BC before the operation, and 748 axillary lymph nodes were detected, all of which were ipsilateral lymph nodes of BC. After pathological study and diagnosis, 540 axillary lymph node metastases were set as lymph node metastasis group, while 208 axillary lymph nodes without metastasis were included in the lymph node non-metastatic group. There was no statistical difference in general data between the two groups of BC patients ($P > 0.05$), so they can be enrolled in this study.

Inclusion criteria

① Patients meet the clinical diagnostic criteria of BC; ② The patients have complete clinical medical records; ③ This study was approved by the hospital's ethics committee. Patients and their families were informed of the purpose and process of this experimental study, and signed an informed consent.

Exclusion criteria

① Patients complicated with brain, heart, kidney, liver and other organ and tissue diseases; ② Patients with mental and other cognitive disorders or patients refusing to cooperate in the study; ③ Patients complicated with systemic coagulation disorder; ④ The clinical data of patients are incomplete.

Methods

Ultrasound diagnostic instrument (Philips iU22), L9-4 Broadband Linear Array Transducer and the contrast software were used with frequency probe of 9.0 MHz and contrast mechanical index of 0.08. Patients kept lying on their backs, with their arms raised and extended outward, exposing their armpits [9-11]. Multiple sections were scanned continuously, and the target lymph nodes were locked in several lymph nodes detected, and one or more clear and meaningful ones in the sonogram were taken for examination [12-14]. The largest long axis section of the lymph node was taken, the probe was kept stable and switched to the contrast mode [15-18]. The 2 ml contrast agent was quickly injected into the elbow vein, followed by injection of 5 ml normal saline, and the section remained unchanged, and the timer was started. The perfusion process of contrast agent was observed continuously for 90 s, and the dynamic whole process of CEUS was stored for subsequent analyses [19-21].

Image analysis

The following indexes were recorded, including BC focus, location, size, aspect ratio, shape, boundary, capsule, internal echo of the focus, internal calcification, peripheral acoustic halo, ratio of cortex to medulla (maximum thickness of cortex to thickness of upper medulla), maximum thickness of cortex, blood flow characteristics of lymph node, contrast perfusion sequence, enhancement features, whether the scope is enlarged after enhancement, whether the boundary is clear, peak intensity, time to peak, area under curve and blood flow signal in lymph nodes. Through semi-quantitative analysis of Alder classification, it can be divided into grade 0, I, II and III. The ultrasonic contrast-enhanced images of axillary lymph nodes were analyzed offline by professional doctors, and the diagnosis results were completed independently. If it is not consistent with the doctor's diagnosis, re-reading the image until an agreement has been reached and then the image can be included in this study.

Statistical analyses

The data obtained in this study were statistically analyzed and processed by SPSS20.0 software. X^2 test was carried out on the count data, expressed as [% (n)]. A *t* test was performed for measurement data, presented as ($x \pm s$). $P < 0.05$ indicated statistically significant differences. Logistic stepwise regression was used to analyze multiple factors.

Results

Comparative analysis of general data of two groups of patients

Table 1 displays that the difference of general data between the two groups did not reach statistical significance.

Univariate correlation analysis between rim enhancement features of CEUS and lymph node metastasis in BC

Correlation between rim enhancement features of CEUS and lymph node metastasis in BC: Whether the boundary is clear after

Table 1. Comparative analysis of general data of two groups of patients

	Lymph node non-metastasis group (n=208)	Lymph node metastasis group (n=540)	*t* or X^2	*P*
Age (years old)	49.1 ± 2.8	48.7 ± 3.4	1.1019	0.2712
Education level			1.7516	0.186
Junior high school and below	39 (18.75%)	73 (13.52%)		
High school and above	169 (81.25%)	467 (86.48%)		
Anamnesis			0.4597	0.498
Hypertension	25 (12.02%)	41 (7.59%)		
Diabetes	22 (10.58%)	63 (11.67%)		
None	161 (77.40%)	436 (80.74%)		
Smoking			0.4365	0.509
Yes	17 (8.17%)	33 (6.11%)		
No	191 (91.83%)	507 (93.89%)		
Alcohol drinking			0.8293	0.362
Yes	63 (30.29%)	139 (25.74%)		
No	145 (69.71%)	401 (74.26%)		
Residence			0.2388	0.625
Town	132 (63.46%)	328 (60.74%)		
Countryside	76 (36.54%)	212 (39.26%)		

enhancement has no statistical significance with lymph node metastasis of BC ($P > 0.05$). Lymph node non-metastasis group had 35 case peripheral halo, 29 case peripheral convergence, 162 case radial enhancement, 171 case homogeneous, 63 case high enhancement, 42 case centripetal, 38 case expanded scope after enhancement; while in the lymph node metastasis group, the number was 456, 123, 236, 69, 364, 427 and 423 respectively. The difference in peripheral halo, peripheral convergence, rim enhancement, enhancement mode, enhancement amplitude, enhancement sequence and expansion after enhancement between the two groups exhibited statistical significance with lymph node metastasis of BC ($P < 0.05$), see **Table 2** for details.

Correlation analysis of peak intensity (PI), time to peak (TTP) and area under curve (AUC) with lymph node metastasis of BC: The PI, TTP and AUC of CEUS were significantly different from those of BC lymph node metastasis ($P < 0.05$), see **Table 3** for details.

Correlation analysis between other related indexes of CEUS and lymph node metastasis of BC: There was no significant difference between the ratio of internal perfusion defect and the ratio of cortex to medulla and lymph node metastasis of BC ($P > 0.05$). Thrombolysis in myocardial infarction (TIMI), perfusion sequence, aspect ratio and maximum cortical thickness were related to lymph node metastasis of BC ($P < 0.05$), see **Table 4** for details.

Logistic stepwise regression analysis

The dependent variable was lymph node metastasis of BC, and the independent variable was a statistically significant index in univariate analysis. Logistic stepwise regression analysis was performed, and the detailed data were shown in **Table 5**. The results showed that enhancement mode, enhancement amplitude, extension after enhancement, maximum cortical thickness, peak intensity and peak time were all related to lymph node metastasis of BC ($P < 0.05$).

Analysis of CEUS features of BC lymph nodes

Female, 45 years old, lymph node metastasis in breast cancer. CEUS shows that the outline of lymphadenography increases significantly and nonhomogeneous enhancement. CEUS shows the cortex becomes thicker when lymph node metastasis occurs, with the maximum thickness exceeding 3 mm. The analysis of CEUS features of BC lymph nodes in this study was shown in **Figure 1**.

Table 2. Correlation between rim enhancement of CEUS and lymph node metastasis of BC

Group	Lymph node non-metastasis group (n=208)	Lymph node metastasis group (n=540)	X^2	*P*
Peripheral halo			311.9846	0.000
Yes	33 (15.87%)	456 (84.44%)		
No	175 (84.13%)	84 (15.56%)		
Peripheral convergence			7.2398	0.007
Yes	29 (13.94%)	123 (22.78%)		
No	179 (86.06%)	417 (77.22%)		
Rim enhancement			70.4652	0.000
Radial enhancement	162 (77.88%)	236 (43.70%)		
Non-radial enhancement	46 (22.12%)	304 (56.29%)		
Enhancement mode			322.2195	0.000
Homogeneous	171 (82.21%)	69 (12.78%)		
Nonhomegeneous	37 (17.78%)	471 (87.22%)		
Enhancement amplitude			64.5369	0.000
High enhancement	63 (30.29%)	364 (67.41%)		
Other enhancement	135 (7.21%)	176 (32.59%)		
Enhancement sequence			222.6093	0.000
Centripetal	42 (20.19%)	427 (79.07%)		
Non-centripetal	166 (79.81%)	113 (20.93%)		
Enhanced boundary			0.3981	0.528
Clear	97 (46.63%)	238 (44.07%)		
Unclear	111 (53.37%)	302 (55.93%)		
Expanded scope after enhancement			229.0899	0.000
Yes	38 (18.27%)	423 (78.33%)		
No	170 (81.73%)	117 (21.67%)		

Table 3. Analysis of PI, TTP and AUC of CEUS in two groups ($\bar{x} \pm s$)

Group	PI	TTP	AUC
Lymph node non-metastasis group (n=208)	5.67 ± 3.79	28.41 ± 17.81	276.29 ± 183.71
Lymph node metastasis group (n=540)	9.02 ± 4.34	22.46 ± 16.05	368.38 ± 214.64
t	9.7866	4.4036	5.4642
P	0.000	0.000	0.000

Discussion

In recent years, the incidence of BC is increasing year by year, which seriously threatens the quality of life and health of women. Lymph node metastasis aggravates BC and is an important indicator for its efficiency of clinical treatment. Doctors are required to make a diagnosis after accurately evaluation of the lymph node metastasis status of BC, and choose the appropriate treatment and prognosis evaluation scheme correspondingly [22, 23]. CEUS is characterized by high accuracy and non-invasion in the examination of BC, which can display the size of the tumor and the shape of the surrounding neovascularization in real time and in a dynamical manner, while the rim enhancement features of CEUS can improve the resolution of contrast-enhanced images, thereby enhancing the accuracy of BC diagnosis [24].

According to this study, peripheral halo, peripheral convergence, rim enhancement, enhancement mode, enhancement amplitude, enhancement sequence, expansion after enhancement, PI, TTP, AUC, TIMI, perfusion sequence, aspect ratio and maximum cortical thickness were all related to lymph node metastasis of BC by uni-

Table 4. Correlation analysis between other indexes of CEUS and lymph node metastasis of BC

Group	Lymph node non-metastasis group (n=208)	Lymph node metastasis group (n=540)	X^2	*P*
TIMI			302.4986	0.000
0-I	41 (19.71%)	465 (86.11%)		
II-III	167 (80.29%)	75 (13.88%)		
Perfusion sequence			20.5730	0.000
Hilar 30 on se	84 (40.38%)	128 (23.71%)		
Cortex (%) n se	124 (59.62%)	412 (76.29%)		
Internal perfusion defect			1.2022	0.273
Yes	73 (35.09%)	213 (39.44%)		
No	135 (64.91%)	327 (60.56%)		
Aspect ratio			163.5407	0.000
< 1.8	137 (65.87%)	95 (17.59%)		
≥ 1.8	71 (34.13%)	445 (82.41%)		
Maximum cortical thickness			85.7201	0.000
≤ 3	126 (60.58%)	133 (24.63%)		
> 3	82 (39.42%)	407 (75.37%)		
Ratio of cortex to medulla			0.4326	0.511
< 1	64 (30.77%)	153 (28.33%)		
≥ 1	144 (69.23%)	387 (71.67%)		

Table 5. Multivariate Logistic stepwise regression analysis of lymph node metastasis of BC

Item	B value	SE	X^2	OR (95% CL)	P
Enhancement mode (nonhomogeneous/homogeneous)	1.025	0.317	22.824	3.805 (2.503-4.972)	< 0.001
Expanded after enhancement (Yes/No)	1.342	0.364	26.507	4.106 (2.845-5.746)	< 0.001
Enhancement amplitude (High/other enhancements)	1.160	0.328	5.133	3.868 (2.517-5.263)	0.008
Maximum cortical thickness (≤ 3 cm/> 3 cm)	0.948	0.315	14.262	3.154 (2.208-4.525)	< 0.001
Peak intensity (High/low)	0.704	0.258	3.925	2.117 (1.805-3.214)	0.026
Time to peak (Long/short)	0.437	0.116	4.208	1.824 (1.526-2.860)	0.017

variate analysis. Multivariate analysis showed that enhancement mode, enhancement amplitude, extension after enhancement, maximum cortical thickness, PI and TTP were all related to lymph node metastasis of BC. From this result, it can be concluded that when doctors perform CEUS examination on patients, the scope expands after enhancement, which indicates the possibility of metastasis of BC lymph nodes. The lymph nodes of metastatic BC are usually nonhomogeneously enhanced, and most of them were accompanied with internal defects, which was largely due to the metastasis of the tumor through the new tiny lymphatic vessels or microvessels around the lymph nodes. The internal defect should be attributed to the fact that the tumor cells directly destroyed or blocked the internal vascular network, resulting in local ischemic necrosis of the internal vascular network. The conclusion of this study was consistent with previous study [25], which supported a correlation between the enhancement mode of BC lymph nodes and axillary lymph node metastasis, while CEUS technology can accurately detect and diagnose BC lymph node metastasis. The metastatic lymph nodes are mainly high enhancement, usually showing marginal or intermediate defects". This conclusion fully proves that the enhanced features of CEUS in BC are related to lymph node metastasis. The limitation of this study is that it did not calculate the sensitivity and specificity of the edge enhancement feature of BC in the diagnosis of lymph node metastasis, and its effectiveness will be further explored in future trials.

To sum up, the rim enhancement features of CEUS have a certain correlation with lymph node metastasis of BC, which can accurately

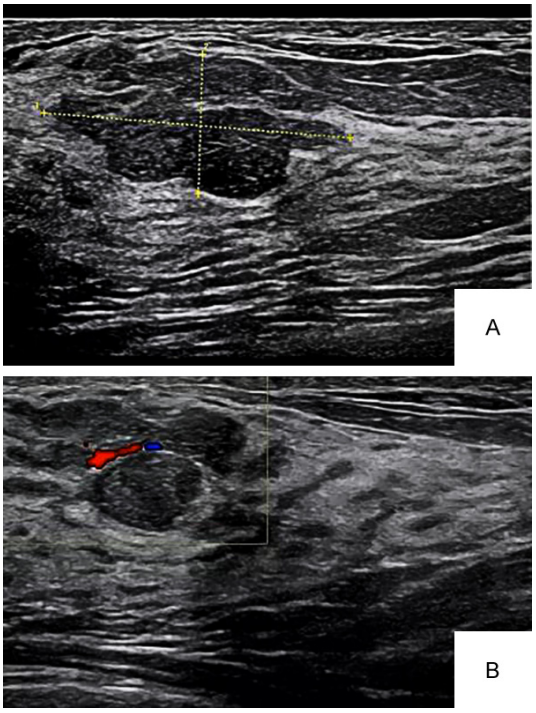

Figure 1. CEUS of BC lymph nodes. Note: (A) Shows that the outline of lymphadenography increases significantly and nonhomogeneous enhancement. (B) Shows that the cortex becomes thicker when lymph node metastasis occurs, with the maximum thickness exceeding 3 mm.

evaluate the growth of microvessels around lymph nodes, provide theoretical basis in the selection of appropriate treatments, with a great value for clinical treatment of BC.

Disclosure of conflict of interest

None.

Address correspondence to: Qiaohong Pan, Department of Ultrasound Medicine, Heping Hospital Affiliated to Changzhi Medical College, 110 South Yanan Road, Changzhi, Shanxi, China. Tel: +86-13834793630; E-mail: PanQiaohong123@126.com

References

[1] Wei S, Zang J, Jia Y, Chen A, Xie Y, Huang J, Li Z, Nie G, Liu H, Liu F and Gao W. A gene-related nomogram for preoperative prediction of lymph node metastasis in colorectal cancer. J Invest Surg 2020; 33: 715-722.

[2] Wang L, Hong Y, Ma J, Han M, Zhang S, Shan B and Liu Y. Combination of pegylated liposomal doxorubicin and docetaxel as neoadjuvant therapy for breast cancer with axillary lymph node metastasis. J Int Med Res 2020; 48: 300060520944310.

[3] Chu Y, Mao T, Li X, Jing X, Ren M, Huang Z, Zhou XB, Chen Y and Tian Z. Predictors of lymph node metastasis and differences between pure and mixed histologic types of early gastric signet-ring cell carcinomas. Am J Surg Pathol 2020; 44: 934-942.

[4] Kurisunkal V, Gulia A, Puri A and Rekhi B. Lymph node metastasis in extremity chondrosarcomas: a series of four cases. South Asian J Cancer 2020; 9: 1-3.

[5] Zenga J, Divi V, Stadler M, Massey B, Campbell B, Shukla M, Awan M, Schultz CJ, Shreenivas A, Wong S, Jackson RS and Pipkorn P. Lymph node yield, depth of invasion, and survival in node-negative oral cavity cancer. Oral Oncol 2019; 98: 125-131.

[6] Zhao W, Wang H, Xie J and Tian B. A clinicopathological study of small lung adenocarcinoma 1 cm or less in size: emphasis on histological subtypes associated with lymph node metastasis and recurrence. Int J Surg Pathol 2020; 28: 579.

[7] Chen J, Zhang D, Fang L, He G and Gao L. Lymph node metastasis in the space between the right carotid artery and jugular vein in papillary thyroid carcinoma. J Int Med Res 2020; 48: 300060520920036.

[8] Lee SY, Yeom SS, Kim CH, Kim YJ and Kim HR. Distribution of lymph node metastasis and the extent of lymph node dissection in descending colon cancer patients. ANZ J Surg 2019; 89: E373-E378.

[9] Hioki M, Ohshita A, Yoshida S, Kanehisa F, Katoh N and Asai J. Pelvic lymph node metastasis in extramammary Paget disease of the scrotum without inguinal lymph node metastasis. Australas J Dermatol 2019; 60: 151-153.

[10] Niikura H, Tsuji K, Tokunaga H, Shimada M, Ishikawa M and Yaegashi N. Sentinel node navigation surgery in cervical and endometrial cancer: a review. Jpn J Clin Oncol 2019; 49: 495-500.

[11] Baker GM, King TA and Schnitt SJ. Evaluation of breast and axillary lymph node specimens in breast cancer patients treated with neoadjuvant systemic therapy. Adv Anat Pathol 2019; 26: 221-234.

[12] Singh S, Shukla S, Singh A, Acharya S, Kadu RP and Bhake A. Comparison of estrogen and progesterone receptor status in tumor mass and axillary lymph node metastasis in patients with carcinoma breast. Int J Appl Basic Med Res 2020; 10: 117-121.

[13] Allard B, Cousineau I, Allard D, Buisseret L, Pommey S, Chrobak P and Stagg J. Adenosine A2a receptor promotes lymphangiogenesis and lymph node metastasis. Oncoimmunology 2019; 8: 1601481.

[14] Wang S, Li F, Qiang D, Hu Z, Meng Y, Shi L, Zhao E and Niu Y. Impact of immunodeficiency on lingual carcinogenesis and lymph node metastasis in mice. J Oral Pathol Med 2019; 48: 826-831.
[15] Hakamivala A, Huang Y, Chang YF, Pan Z, Nair A, Hsieh JT and Tang L. Development of 3D lymph node mimetic for studying prostate cancer metastasis. Adv Biosyst 2019; 3: e1900019.
[16] Liang X, Li Z, Zhang L, Wang D and Tian J. Application of contrast-enhanced ultrasound in the differential diagnosis of different molecular subtypes of breast cancer. Ultrason Imaging 2020; 42: 261-270.
[17] Liu G, Wang ZL, Zhang MK, He Y and Liu Y. Breast hamartoma: ultrasound, elastosonographic, and contrast-enhanced ultrasound features. J Cancer Res Ther 2019; 15: 864-870.
[18] Mann RM, Kuhl CK and Moy L. Contrast-enhanced MRI for breast cancer screening. J Magn Reson Imaging 2019; 50: 377-390.
[19] Lee SC, Tchelepi H, Grant E, Desai B, Luo C, Groshen S and Hovanessian-Larsen L. Contrast-enhanced ultrasound imaging of breast masses: adjunct tool to decrease the number of false-positive biopsy results. J Ultrasound Med 2019; 38: 2259-2273.
[20] Lee JO, Kang MJ, Byun WS, Kim SA, Seo IH, Han JA, Moon JW, Kim JH, Kim SJ, Lee EJ, In Park S, Park SH and Kim HS. Metformin overcomes resistance to cisplatin in triple-negative breast cancer (TNBC) cells by targeting RAD51. Breast Cancer Res 2019; 21: 115.
[21] Dong T. Early response assessed by contrast-enhanced ultrasound in breast cancer patients undergoing neoadjuvant chemotherapy. Ultrasound Q 2018; 34: 84-87.
[22] Zhong J, Sun DS, Wei W, Liu X, Liu J, Wu X, Zhang Y, Luo H and Li Y. Contrast-enhanced ultrasound-guided fine-needle aspiration for sentinel lymph node biopsy in early-stage breast cancer. Ultrasound Med Biol 2018; 44: 1371-1378.
[23] Wan CF, Liu XS, Wang L, Zhang J, Lu JS and Li FH. Quantitative contrast-enhanced ultrasound evaluation of pathological complete response in patients with locally advanced breast cancer receiving neoadjuvant chemotherapy. Eur J Radiol 2018; 103: 118-123.
[24] Sorin V, Yagil Y, Yosepovich A, Shalmon A, Gotlieb M, Neiman OH and Sklair-Levy M. Contrast-enhanced spectral mammography in women with intermediate breast cancer risk and dense breasts. AJR Am J Roentgenol 2018; 211: W267-W274.
[25] Liu GF, Wang ZQ, Zhang SH, Li XF, Liu L, Miao YY and Yu SN. Diagnostic and prognostic values of contrast-enhanced ultrasound combined with diffusionweighted magnetic resonance imaging in different subtypes of breast cancer. Int J Mol Med 2018; 42: 105-114.